

9. TEXTURAL ANALYSES OF VEIN NETWORKS AND SULFIDE IMPREGNATION ZONES: IMPLICATIONS FOR THE STRUCTURAL DEVELOPMENT OF THE BENT HILL MASSIVE SULFIDE DEPOSIT¹

L. Lynn Marquez² and Pierre Nehlig³

ABSTRACT

During Leg 169, we recovered core from massive sulfide and the underlying sulfide feeder system of two massive sulfide deposits, the Bent Hill Massive Sulfide and the Ore Drilling Program Mound. Veins and impregnation zones of these deposits record the structural evolution of the mound and the pathways of hydrothermal fluid flow. Sulfides in the feeder system are found either as veins that typically display one episode of mineral infilling or as precipitates within the primary sedimentary pore structure. Sulfide veining is most abundant within the mud-rich units, whereas sulfide infilling of pore spaces is most common within sandy units. Sulfide veins generally crosscut the primary sedimentary structures at right angles. These observations suggest a simple model of hydrothermal fluid flow. Hydrothermal fluids are first transported from depth via focused fluid flow. Within 200 to 300 m of the surface, these fluids exit the conduit and enter sandy turbidite layers. Conductive cooling of the fluid results in the precipitation of sulfides within the sedimentary pore structure. Precipitation, in turn, inhibits additional permeable fluid flow, thereby causing fluid pressures to increase and effective pressure to decrease. This pressure regime favors the creation of subvertical fracture networks that may transport hydrothermal fluids across more impermeable mud-rich layers. Upward transport of fluids across impermeable layers may also occur through open frac-

¹Marquez, L.L., and Nehlig, P., 2000. Textural analyses of vein networks and sulfide impregnation zones: implications for the structural development of the Bent Hill Massive Sulfide deposit. In Zierenberg, R.A., Fouquet, Y., Miller, D.J., and Normark, W.R. (Eds.), *Proc. ODP, Sci. Results*, 169, 1–25 [Online]. Available from World Wide Web: <http://www-odp.tamu.edu/publications/169_SR/VOLUME/CHAPTERS/SR169_09.PDF>. [Cited YYYY-MM-DD]

²Department of Earth Sciences, PO Box 1002, Millersville University of Pennsylvania, Millersville PA 17551-0302, USA.

marquez@rain.millersv.edu

³Bureau de Recherches Géologiques et Minières, B.P. 6009, 45060 Orleans cedex, France.

Date of initial receipt: 3 March 1999

Date of acceptance: 25 April 2000

Date of publication: 15 August 2000

Ms 169SR-118

tures created by tectonic stresses at the ridge. Horizontal permeable flow through sandy units and focused vertical flow through mud-rich units over extended periods of time can create the underlying feeder system that may eventually result in massive sulfide.

INTRODUCTION

Core drilled during Leg 169 provides a remarkable opportunity to characterize and evaluate the structural evolution of a massive sulfide mound. To determine the lateral extent of mineralization and to characterize the sulfide system with depth, we drilled along a north-south and an east-west transect and drilled through the apex of the Bent Hill Massive Sulfide (BHMS) to a depth of 500 m. At this depth, basalt flows interpreted as volcanic basement were recovered (Fouquet, Zierenberg, Miller, et al., 1998). Both the massive sulfide and the underlying sulfide feeder systems were successfully recovered in three holes, providing an outstanding sequence of core with which to analyze the structural mechanisms for massive sulfide formation at sedimented ridges.

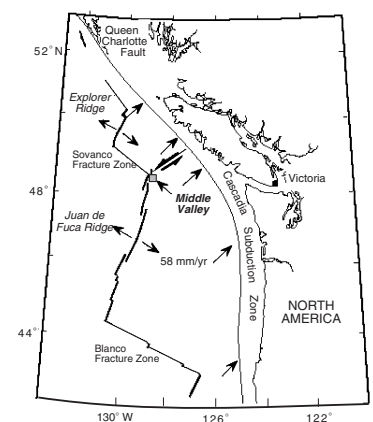
Previously, studies of sedimented-covered ridge sulfide mounds have concentrated on the composition of the sulfides to constrain the genesis of the sulfide system (Ames et al., 1993; Goodfellow and Franklin, 1993; Butterfield et al., 1994; Campbell et al., 1994; Davis and Fisher, 1994; Duckworth et al., 1994; Zierenberg et al., 1994). Equally as important, however, are studies that attempt to characterize the structural evolution of the sulfide mound. Economic geologists have long recognized the importance of understanding the structure of the hydrothermal system to explore economic grade ores. Unfortunately, the poor recovery of densely fractured materials from the ocean crust has significantly reduced the feasibility of structural studies in active seafloor deposits. Therefore, the study of the structural evolution of sulfide mounds on the seafloor has largely been limited to information obtained through seismic analyses (Macdonald and Luyendyk, 1977; Karson and Rona, 1990; Davis et al., 1992; Davis and Villinger, 1992; Davis and Becker, 1994). One viable means by which the structural framework of massive sulfide deposits can be constrained has largely been ignored in drilled core. Vein textures provide a valuable record of the pathways by which hydrothermal fluids flow. This paper derives a model of hydrothermal circulation at the BHMS deposit based upon vein fabrics and infilling textures in the sulfide feeder system of the BHMS deposit.

GEOLOGY OF MIDDLE VALLEY

Middle Valley, Juan de Fuca Ridge, is an intermediate rate (58 mm/yr) spreading center that forms the ridge component of a ridge-transform-transform unstable triple junction (Fig. F1) (Davis and Villinger, 1992). Reduced magma supply along the Juan de Fuca Ridge has resulted in a ridge morphology that more closely resembles a slow-spreading center (Davis and Villinger, 1992). The ridge is buried by 200 to >1000 m of turbiditic sands and hemipelagic sediments supplied during the Pleistocene glacial low stand of sea level.

Two areas of venting at Middle Valley, the area of active venting (AAV) and Bent Hill, were drilled during Leg 169. This paper deals only with the Bent Hill locality because these cores recovered not only mas-

F1. Tectonic setting of Middle Valley sedimented ridge, p. 12.



sive sulfide but also the underlying sulfide feeder system. Both the AAV and Bent Hill are located between the north-south trending rift-bounding faults located ~15 km apart. Bent Hill lies ~3 km west of the eastern bounding fault and is one of several linear mounds that parallel the eastern normal fault scarp (Mottl, Davis, Fisher, and Slack, 1994). A ridge-parallel normal fault underlies the western edge of the BHMS and the hills that lie farther south (Goodfellow and Franklin, 1993; Davis et al., 1992). The BHMS deposit lies ~100 m south of Bent Hill (Fig. F2), is ~35 m high, extensively weathered to iron oxyhydroxides, and partially buried by sediment.

The second sulfide mound (Ore Drilling Program Mound [ODP Mound]) is ~330 m south of the BHMS mound and lies along the same north-south trending fault that underlies Bent Hill. ODP Mound is actually two adjacent 12-m mounds. It is believed that ODP Mound is younger than the BHMS because of the lack of sediment cover and limited oxidation of the sulfide phases (Fouquet, Zierenberg, and Miller, et al., 1998). One 264°C hydrothermal vent is present on the northern flank of the deposit (Davis and Villinger, 1992).

DRILL HOLE AND SAMPLE SELECTION

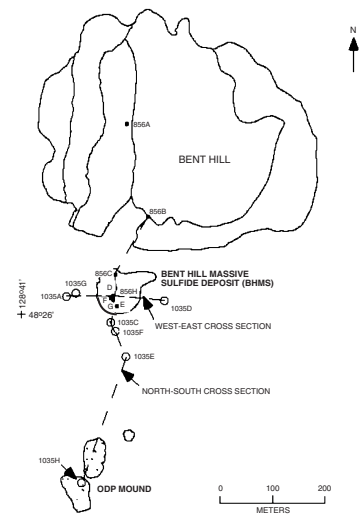
One can characterize the evolution of the fluid regime and the structural characteristics of sulfide mound genesis through the study of hydrothermal vein textures in a massive sulfide deposit. This paper describes the hydrothermal system as evident from the infilling, replacement, and vein textures of the core recovered from three holes: Holes 856H, 1035F, and 1035H (Fig. F3). These are the three deepest holes drilled in the Bent Hill area that penetrated and recovered the underlying sulfide feeder system. Hole 856H extends to a depth of 500 m and was drilled through the center of the BHMS. Hole 1035F was drilled ~100 m south of the BHMS and extends to a depth of ~230 m. Hole 1035H, located at the center of ODP Mound, extends to a depth of ~245 m.

Twenty-five samples were selected for this study from the massive sulfide and sulfide feeder zones of Holes 856H, 1035F, and 1035H to evaluate the formation of veins and impregnation zones that feed the sulfide system. Sulfide impregnated samples exhibit a range of mineralization that includes bedding-parallel infilling as well as densely packed sulfide disseminations. Sulfide veined samples exhibit single veins, vein networks, and vein networks with sulfide impregnation zones. Those samples with crosscutting vein networks and sulfide impregnation zones were especially relevant to this study to constrain the relationship between horizontal and vertical fluid flow. Samples of veins and impregnation textures were selected throughout the core. However, where possible, multiple samples were collected within a 1- to 2-m interval of the core to evaluate textures generated within the same lithology and stress regime. Although this sampling scheme does not guarantee the same stress conditions, the likelihood of similar physical conditions is increased. This becomes important when creating a structural model based on limited exposure in drilled core.

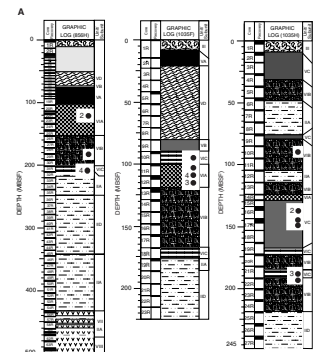
HOLE STRATIGRAPHY

The Bent Hill drill holes followed a generalized stratigraphy from the surface to depth as follows: clastic sulfide, massive sulfide, sulfide feeder

F2. Location of Bent Hill and ODP Mound drill holes from Legs 139 and 169, p. 13.



F3. Log of Holes 856H, 1035F, and 1035H, p. 14.



system with an underlying deep copper zone (DCZ), sediments, and basaltic sill and flow complex (Fig. F3). Each group has been further subdivided into subunits that are described in the Leg 169 *Initial Reports* volume (Fouquet, Zierenberg, Miller, et al., 1998). Because this paper details the evolution of the sulfide feeder units, these units will be described below. In the Leg 169 *Initial Reports*, the sulfide feeder system, Unit VI, is divided in three subunits based on the degree of sulfide mineralization (Fouquet, Zierenberg, Miller, et al., 1998). Subunit VIA is sulfide-veined sediment where sulfides are predominant in the veins but are also present as fine-grained disseminations. The total sulfide content in Subunit VIA ranges from 10 to 50 vol%. The major sulfides in these units are isocubanite, chalcopyrite, pyrrhotite, with minor pyrite and traces of marcasite and galena. Subunit VIB is defined as sediment with sulfide veins and/or impregnations. This unit is only weakly mineralized, and the dominant sulfides are pyrrhotite, chalcopyrite/isocubanite, and pyrite with minor sphalerite. The sulfide mineralogy is not consistent in this unit and may change from section to section downhole. The final subunit in the sulfide feeder system, Subunit VIC, is characterized by sulfide bands and impregnations in sandstone. This unit is predominantly CuFe-sulfide rich, and sulfides commonly mimic primary sedimentary structures. A DCZ falls within this subunit and is identified by a predominance of CuFe sulfides and the relative absence of any other sulfide minerals.

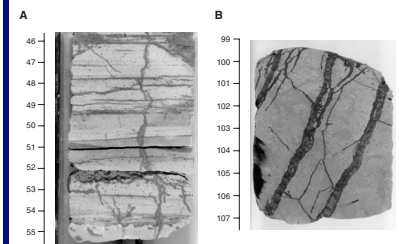
SAMPLE DESCRIPTION

Sulfide Feeder System Unit VIA

Subunit VIA is characterized by sulfide veins and minor sulfide disseminations. Ten samples from Subunit VIA were chosen for thin-section analysis: two from Hole 856H and eight from Hole 1035F. Two distinctive textures are evident within these samples: sulfide infilling of sedimentary features and subvertical sulfide veins (Fig. F4). Within the samples studied, pyrrhotite and chalcopyrite most commonly infill sedimentary pore structures. Euhedral pyrite crystals and minor (<5%) magnetite are common and generally present with chalcopyrite. Chalcopyrite is also present as a secondary mineral adjacent to pyrrhotite. In Hole 1035F, sulfide infilling of sedimentary pore spaces is similar; however, unlike the samples from Hole 856H, vein assemblages are more common than disseminated sulfide. Most of the disseminated sulfide in Hole 1035F is present as chalcopyrite impregnations (~0.5 mm). Magnetite (modal abundance of 5%–10%) is commonly found along vugs and near chalcopyrite in ~0.2-mm subhedral crystals. In interval 169-1035F-12R-1, 78–93 cm, disseminations are primarily pyrrhotite with minor pyrite alteration rims, as opposed to chalcopyrite disseminations previously described. In summary, the sulfide textures in Subunit VIA in both Holes 856H and 1035F are characterized by pyrrhotite and chalcopyrite infilling or replacement of the primary sedimentary texture.

Subvertical sulfide veins comprise the second dominant sulfide texture within Subunit VIA. Two types of veins are within this subunit. Veins in Subunit VIA of Hole 856H are characterized by Mode 1 extension fractures with one mineralization event, often evidenced by syntaxial textures. Secondary alteration of sulfide phases may occur subsequent to mineral infilling. Hole 1035F also has extension veins characterized by a single episode of mineral infilling, but multiple-

F4. Samples of pyrrhotite and sphalerite veins and pyrrhotite-sphalerite-chalcopyrite veins, p. 16.



event sulfide veins are also present. Multiple stages of fluid flow are evidenced by classic crack-seal textures and crosscutting networks of multiple narrow veins.

Veins in Hole 856H perpendicularly crosscut the bedding-parallel sulfide-impregnated layers. Typically, veins in Hole 856H are composed of pyrite with lesser amounts (<5%) of magnetite. Chalcopyrite commonly rims pyrite crystals. Pyrrhotite is also present at the rim of some pyrite veins. In Sample 169-856H-21R-1, 96–97 cm, the crosscutting vein is linked with a horizontal vein. The vertical and horizontal veins have a similar composition: pyrrhotite crystals (0.75–1.0 mm) with secondary Fe silicates along the cleavage traces and subhedral to euhedral sphalerite with pyrite.

In Core 169-1035F-11R, extension veins are lined with euhedral quartz crystals, whereas the interiors of the veins are infilled with sulfides (Fig. F5). The quartz-lined fractures are infilled with pyrrhotite (80%–90%), chalcopyrite (8%–15%), and magnetite (2%–5%). Many of these veins exhibit a distinctive Fe silicate alteration halo, and the sediments surrounding the veins are typically chloritized. These sections have a modal abundance of 20%–25% sulfide since sulfides are found not only within the veins but also as dissemination within the section.

Starting in Core 169-1035F-12R, the vein assemblages become more complex. Infilling of extension fractures remains the dominant vein formation mechanism; however, at least four sulfide phases exist within the veins, and anhydrite borders the vein (Fig. F6). Veins in this core are composed of pyrrhotite, sphalerite, pyrite, and chalcopyrite. Pyrrhotite is present as distinctive 0.1- to 0.25-mm crystals with Fe silicate alteration along the cleavage traces. Pyrite is present as subhedral to euhedral cubic crystals in larger veins (aperture of 1–2 mm), and in euhedral crystals with chalcopyrite and minor sphalerite in narrower (aperture <0.5 mm) and later veins. The other primary sulfide assemblage within this core is chalcopyrite, present as blebs and inclusions within the altered sediment (Fig. F7). The larger veins in Sample 169-1035F-12R-1, 39–42 cm, exhibit a greater degree of alteration, which is consistent with the presence of anhydrite vein selvages bordering the veins. The anhydrite vein selvages extend 0.5 to 1.0 mm from the vein and are subhedral to euhedral anhydrite blades. Throughout this core, anhydrite is bladed and radiating, suggesting renewed hydrothermal fluid flow since sulfate is not stable at the high temperatures consistent with the vein sulfides.

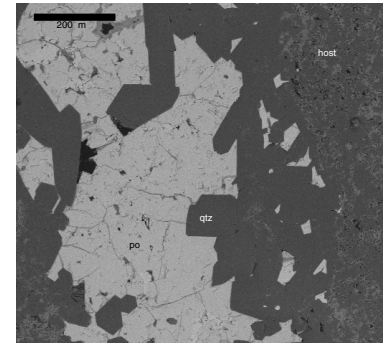
In summary, the sequence of sulfide deposition within the sulfide veined sediments in Holes 856H and 1035F are as follows:

1. Pyrrhotite precipitation in sediments (with lesser amounts of chalcopyrite, magnetite, and rare euhedral quartz) primarily within pore spaces; and
2. Pyrite and chalcopyrite veins that crosscut pyrrhotite infilling and replacement textures. It is important to note that the most complicated (e.g., multiphase) vein assemblages also have the most complex alteration history and exhibit distinctive anhydrite vein selvages.

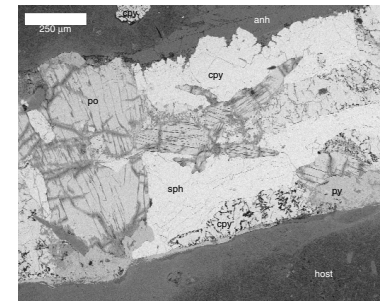
Subunit VIB

Subunit VIB is composed of sediment with 2–10 vol% sulfide veins and/or impregnations (Fig. F8). The total sulfide content is less in this subunit than in Subunit VIA. Three samples were chosen from this unit:

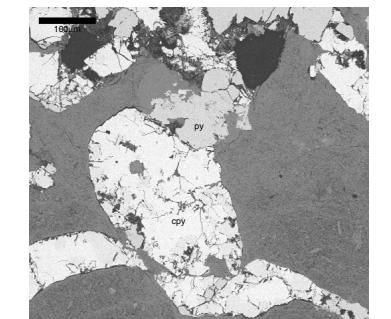
F5. Backscattered electron image of quartz-lined extension fracture infilled by pyrrhotite, p. 17.



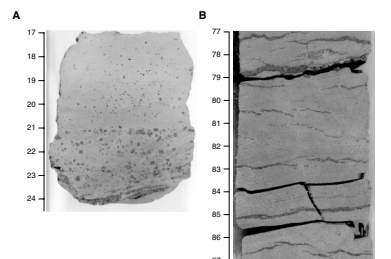
F6. Backscattered image of sulfide vein assemblage, p. 18.



F7. Backscattered electron image of chalcopyrite blebs and veins in sulfide-veined sediment, p. 19.



F8. Subunit VIB siltstone and chalcopyrite in fine-grained sandstone, p. 20.



one from Hole 856H and two from Hole 1035H. The host sediments are typically altered to fibrous chlorite (needles <0.1 mm in length) that overgrows quartz grain boundaries. Quartz comprises ~40% of these sections.

Two types of sulfide deposition, similar to those found in Subunit VIA, also are within these samples. Chalcopyrite is present as both small (<0.2 mm) impregnations in sediment and as subvertical veins. This is in contrast to the veins in Subunit VIA, which are dominantly pyrite or pyrrhotite. The concentration of chalcopyrite disseminations in sediment decreases away from the subvertical veins. This is in contrast to the vein patterns evident in Subunit VIA, where there is no correlation between disseminated sulfide concentration and proximity to the vein.

Subunit VIC

The final sulfide feeder unit is the sulfide-banded and impregnated sediments where sulfides comprise 10–50 vol% of the core (Fig. F9). Eight thin sections were studied from Holes 856H and 1035H. Bands of chalcopyrite/isocubanite, which parallel sedimentary bedding, characterize these samples. Sulfide bands have either equant grain boundaries or rounded grain boundaries that result from alteration of the sulfide phases. Chalcopyrite is found with euhedral quartz and minor pyrrhotite and generally precipitates within the primary sedimentary pore spaces (Fig. F10).

In Hole 1035H, the sulfide bands are composed of predominantly cubic pyrite crystals 0.75–1.5 mm in size. The pyrite bands comprise ~50% of the opaque phases. Pyrrhotite stringers found throughout the pyrite have apertures of <0.1 mm and comprise ~15% of the opaque phases. Pyrrhotite is also found along the edges of the pyrite cubes (Fig. F11). Hematite commonly is found at the center of the veins and within large pyrite crystals. Hematite, as an alteration product, comprises ~30% of many samples. Narrow (<0.2 mm) veins of sphalerite and magnetite crosscut pyrite. Deeper within Hole 1035H (Core 21R), sulfide bands composed of chalcopyrite/isocubanite precipitated in the primary sedimentary pore structure.

In summary, the sulfide-banded unit is characterized by chalcopyrite/isocubanite banding that infills the primary sedimentary pore structure. Quartz and pyrrhotite are common, whereas sulfides contemporaneous with chalcopyrite are less abundant.

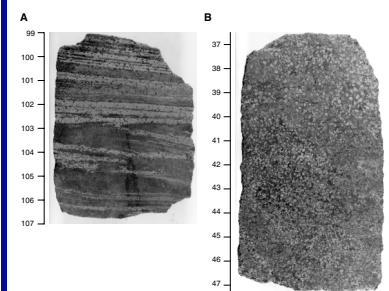
In contrast, pyrite is the dominant sulfide phase and pyrrhotite stringers crosscut and replace pyrite within Core 169-1035H-17R.

DISCUSSION

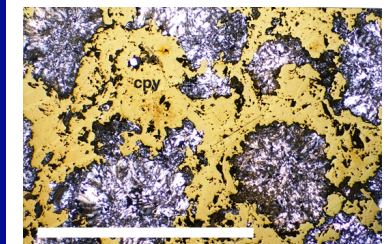
Two questions must be answered to address how structures affect the flow of hydrothermal fluids through the sediment pile to create massive sulfide mounds. The first question concerns the geochemistry of the sulfides and whether hydrothermal fluids interacted extensively with the sediment or whether a distinct basalt signature remains in the system. The second question answers more specifically how the sulfide feeder units are created and how they result in massive sulfide mounds.

Geochemical signatures of the BHMS indicate a basalt source modified by reaction with sediments (Goodfellow and Franklin, 1993; Zierenberg et al., 1993). Permeable flow of hydrothermal fluid through 500

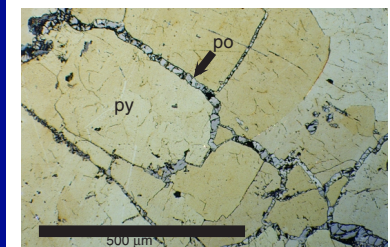
F9. Subunit VIC Cu-rich sulfide-banded cross-laminated sandstone and sulfide-banded sandstone, p. 21.



F10. Chalcopyrite precipitation within sedimentary pore spaces, p. 22.



F11. Pyrrhotite replacement along pyrite grain boundaries, p. 23.



m (depth to basalt basement identified in Hole 856H) of sediment would likely result in a geochemical signature more like Escanaba Trough sulfides, which indicate a greater sediment component (Goodfellow and Franklin, 1993; Zierenberg et al., 1993). Because the sulfides in the BHMS do have an intermediate basalt signature, focused fluid flow must be invoked to transport hydrothermal fluid from depth. This idea, that focused fluid flow is required to produce massive sulfide deposits, is supported by physical evidence such as hydrothermal vent fields forming at the intersections of faults (Rona and Clague, 1989). In addition, thermal models based on massive sulfide deposition also suggest that focused fluid flow is required to rapidly advect heat and transport metals to the surface (Fehn and Cathles, 1979; Strens and Cann, 1982; Lowell and Rona, 1985).

Even though thermal models of massive sulfide deposition require focused fluid flow, and the geochemical signatures of the BHMS deposit suggest focused fluid flow, no fault zone or permeable vertical horizon was recovered during drilling of Leg 169. However, this does not require that fluid flow be governed by porous flow from depth. Indirect evidence exists for the presence of a hydrothermal conduit, possibly a fault, that transports fluid from basement to the sediment layers near the surface. First, the Bent Hill series of mounds follow the trend of a normal fault that offsets basement reflectors but does not intersect the uppermost sediment layers (Davis and Villinger, 1992; Davis, Mottl, Fisher, et al., 1992). Even though the fault may now be inactive, as suggested by the lack of offset in the uppermost sedimentary layers, the fault may represent an open conduit for fluid flow. Second, downhole logging of Hole 856H indicates that a fault may have been intersected at a depth of 221–239 meters below seafloor (mbsf) and/or 250–270 mbsf (Fouquet, Zierenberg, Miller, et al., 1998). Within these intervals, low resistivity and high porosity were recorded, which suggest increased permeability. These zones also coincide with particularly low core recovery (~7%) and a change in pore-fluid chemistry (Fouquet, Zierenberg, Miller, et al., 1998). Third, the distinct lack of vertical or subvertical veining and the predominance of horizontal replacement in units such as the DCZ would suggest that the primary permeable horizon in these units is horizontal and that fluids were not flowing up through and across these horizons but, rather, were flowing along the horizon. These textures would indicate that hydrothermal fluids flowed into permeable layers from a conduit rather than flowing into the horizon from below through distributed porous flow. And finally, the very nature of ocean drilling precludes the intersection of near-vertical fault conduits. A near-vertical drill string is unlikely to intersect a near-vertical fault. Furthermore, the friable nature of brittle fault material reduces the likelihood of recovering the fault material even if a fault were intersected.

Whereas no direct evidence exists for a fault that transmits sulfide depositing hydrothermal fluids from depth, direct evidence does exist for horizontal flow of hydrothermal fluids through the sediments and limited vertical transport of fluid through veins. Evidence includes the dominant sulfide textures—sulfide precipitation within the primary sedimentary pore structure and subvertical vein networks that generally crosscut the horizontal sedimentary (and sulfide) fabric. Regardless of what subunit in the sulfide feeder system is studied, the infiltration and vein textures remain remarkably similar even if the sulfide mineralogy differs. This indicates that the same structural mechanisms are at work throughout the feeder system. It should also be noted that sulfide infill-

ing of pore spaces, especially those of Subunit VIC, are predominantly found within coarser grained sediments, whereas the sulfide-veined units are predominantly in the mud to siltstones (Fig. F12).

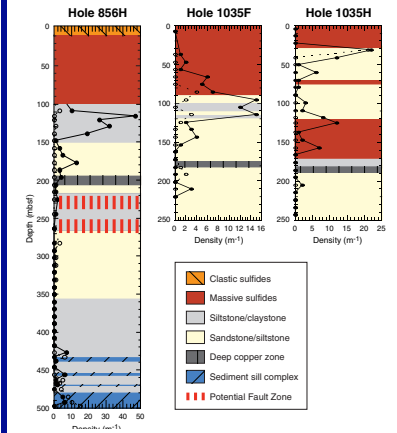
A simple model, similar to one proposed by Zierenberg et al. (1993) for fluid flow in clastic sulfides, can be proposed for the structural evolution of and hydrothermal circulation within the BHMS. Hydrothermal fluids are transported away from a hydrothermal conduit, most likely a fault, along permeable sandy turbidite layers. As the hydrothermal fluids conductively cool, they precipitate sulfides within the pore spaces of the sediments, similar to models of sulfide deposition proposed for stratiform copper deposits (Fox, 1984; Brown, 1992). Hydrothermal fluids are confined to permeable horizons by the mud- and clay-rich layers that bound them. If sulfide precipitation effectively inhibits further permeable fluid flow, fluid pressures may become elevated within the sandy horizons. As fluid pressure increases, the effective pressure in the unit decreases, thereby initiating fracturing (Phillips, 1972; Cox et al., 1995). Once fractures open, hydrothermal fluids will be drawn into the crack through the induced pressure gradient, where they will then probably precipitate sulfides (Etheridge et al., 1984). If the crack remains open, fluids may flow through the fracture network from one permeable horizon to the next. This mechanism most likely operates only at a small scale between narrow horizons and does not act as the dominant fluid transport mechanism (Fig. F13). This statement is supported by the fact that most subvertical veins exhibit only one sequence of hydrothermal precipitate, rather than multistage mineralization. Additional evidence that precipitation of hydrothermal minerals in permeable horizons creates pressure regimes capable of inducing fracture is that most subvertical sulfide veins crosscut the horizontal sulfide impregnation textures. This indicates that horizontal fluid flow came first. Only rarely do subvertical veins directly feed a horizontal vein.

In addition to flow through fractures created by induced pressure regimes, vertical transport of hydrothermal fluids may occur through fracture networks created by tectonic stresses at the ridge. If these fractures remain open, they would provide an obvious pathway for hydrothermal fluids. This mechanism is preferred for the few centimeter-wide veins recovered in the drilled cores that showed evidence for multiple episodes of vein filling. The limited recovery of large aperture subvertical sulfide veins that transmit fluids between permeable horizons may be explained by the sampling bias of vertically drilled cores. It is likely that many more of these veins exist within the sulfide mound and do successfully transport fluids from one permeable horizon to the next, but the bias of the drilled cores precludes their recovery.

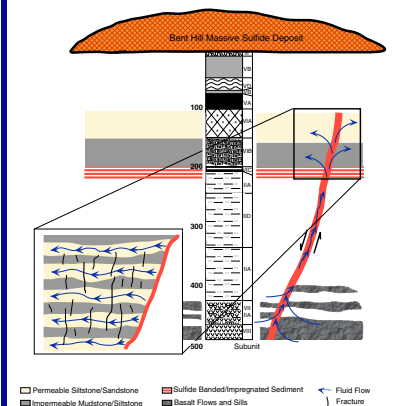
CONCLUSIONS

The sulfide textures of the BHMS deposit feeder system suggest a simple system where hydrothermal fluids were first transported from basement via a fault conduit (Fig. F13). From the conduit, hydrothermal fluids entered the sediment system along permeable sandy turbidite layers. These fluids then precipitated chalcopyrite and pyrrhotite as they cooled. Less permeable mud- and clay-rich layers effectively confined sulfide deposition to sedimentary pore spaces within the permeable sandy units. Sulfide veining in the mud-rich sediments resulted from elevated fluid pressures induced by sulfide precipitation within

F12. Vein density with depth and the representative lithology of the host rock, p. 24.



F13. Hydrothermal circulation model, p. 25.



the sandy units or by fluid flow through existing fracture networks. Most subvertical veins provided only limited hydrothermal fluid transport, but several centimeter-wide, multistage sulfide veins provide evidence for effective transport of fluids vertically through the sediment pile. Continued precipitation of sulfides within the permeable units and within veins of the impermeable units resulted in the well-developed feeder system at Bent Hill.

REFERENCES

- Ames, D.E., Franklin, J.M., and Hannington, M.H., 1993. Mineralogy and geochemistry of active and inactive chimneys and massive sulfide, Middle Valley, northern Juan de Fuca Ridge: an evolving hydrothermal system. *Can. Mineral.*, 31:997–1024.
- Brown, A.C., 1992. Sediment-hosted stratiform copper deposits. *Geosci. Can.*, 119:124–141.
- Butterfield, D.A., McDuff, R.E., Franklin, J., and Wheat, C.G., 1994. Geochemistry of hydrothermal vent fluids from Middle Valley, Juan de Fuca Ridge. In Mottl, M.J., Davis, E.E., Fisher, A.T., and Slack, J.F. (Eds.), *Proc. ODP, Sci. Results*, 139: College Station, TX (Ocean Drilling Program), 395–410.
- Campbell, A.C., German, C.R., Palmer, M.R., Gamo, T., and Edmond, J.M., 1994. Chemistry of hydrothermal fluids from the Escanaba Trough, Gorda Ridge. In Morton, J.L., Zierenberg, R.A., Reiss, C.A. (Eds.), *Geologic, Hydrothermal, and Biologic Studies at Escanaba Trough, Gorda Ridge, Offshore Northern California*. U.S. Geol. Surv. Bull., 2022:201–221.
- Cox, S.F., Sun, S.S., Etheridge, M.A., Wall, V.J., and Potter, T.F., 1995. Structural and geochemical controls on the development of turbidite-hosted gold quartz vein deposits, Wattle Gully Mine, Central Victoria, Australia. *Econ. Geol.*, 90:1722–1746.
- Davis, E.E., and Becker, K., 1994. Thermal and tectonic structure of the Escanaba Trough: new heat-flow measurements and seismic-reflection profiles. In Moreton, J., Zierenberg, R.A., and Reiss, C.A. (Eds.), *Geologic, Hydrothermal, and Biologic Studies at Escanaba Trough, Gorda Ridge, Offshore Northern California*. U.S. Geol. Surv. Bull., 2022:45–64.
- Davis, E.E., Chapman, D.S., Mottl, M.J., Bentkowski, W.J., Dadey, K., Forster, C., Harris, R., Nagihara, S., Rohr, K., Wheat, G., and Whiticar, M., 1992. FlankFlux: an experiment to study the nature of hydrothermal circulation in young oceanic crust. *Can. J. Earth Sci.*, 29:925–952.
- Davis, E.E., and Fisher, A.T., 1994. On the nature and consequences of hydrothermal circulation in the Middle Valley sedimented rift: inferences from geophysical and geochemical observations, Leg 139. In Mottl, M.J., Davis, E.E., Fisher, A.T., and Slack, J.F. (Eds.), *Proc. ODP, Sci. Results*, 139: College Station, TX (Ocean Drilling Program), 695–717.
- Davis, E.E., Mottl, M.J., Fisher, A.T., et al., 1992. *Proc. ODP, Init. Repts.*, 139: College Station, TX (Ocean Drilling Program).
- Davis, E.E., and Villinger, H., 1992. Tectonic and thermal structure of the Middle Valley sedimented rift, northern Juan de Fuca Ridge. In Davis, E.E., Mottl, M.J., Fisher, A.T., et al., *Proc. ODP, Init. Repts.*, 139: College Station, TX (Ocean Drilling Program), 9–41.
- Duckworth, R.C., Fallick, A.E., and Rickard, D., 1994. Mineralogy and sulfur isotopic composition of the Middle Valley massive sulfide deposit, northern Juan de Fuca Ridge. In Mottl, M.J., Davis, E.E., Fisher, A.T., and Slack, J.F. (Eds.), *Proc. ODP, Sci. Results*, 139: College Station, TX (Ocean Drilling Program), 373–385.
- Etheridge, M.A., Wall, V.J., Cox, S.F., and Vernon, R.H., 1984. High fluid pressures during regional metamorphism and deformation: implications for mass transport and deformation mechanisms. *J. Geophys. Res.*, 89:4344–4358.
- Fehn, U., and Cathles, L.M., 1979. Hydrothermal convection at slow-spreading mid-ocean ridges. *Tectonophysics*, 55:239–260.
- Fouquet, Y., Zierenberg, R.A., Miller, D.J., et al., 1998. *Proc. ODP, Init. Repts.*, 169: College Station, TX (Ocean Drilling Program).
- Fox, J.S., 1984. Beshi-type volcanogenic sulphide deposits: a review. *CIM Bull.*, 77:57–68.
- Goodfellow, W.D., and Franklin, J.M., 1993. Geology, mineralogy and chemistry of sediment-hosted clastic massive sulfides in shallow cores, Middle Valley, northern Juan de Fuca Ridge. *Econ. Geol.*, 88:2033–2064.

- Karson, J.A., and Rona, P.A., 1990. Block tilting, transfer faults, and structural control of magmatic and hydrothermal processes in the TAG area, Mid-Atlantic Ridge 26°N. *Geol. Soc. Am. Bull.*, 102:1635–1645.
- Lowell, R.P., and Rona, P.A., 1985. Hydrothermal models for the generation of massive sulfide ore deposits. *J. Geophys. Res.*, 90:8769–8783.
- Macdonald, K.C., and Luyendyk, B.P., 1977. Deep-tow studies of the structure of the Mid-Atlantic Ridge crest near 37°N (FAMOUS). *Geol. Soc. Am. Bull.*, 88:621–636.
- Mottl, M.J., Davis, E.E., Fisher, A.T., and Slack, J.F. (Eds.), 1994. *Proc. ODP, Sci. Results*, 139: College Station, TX (Ocean Drilling Program).
- Phillips, W.J., 1972. Hydraulic fracturing and mineralization. *J. Geol. Soc. London*, 128:337–359.
- Ribando, R.J., Torrance, K.E., and Turcotte, D.L., 1976. Numerical models for hydrothermal circulation in the oceanic crust. *J. Geophys. Res.*, 81:3007–3012. [AUTHOR: Not cited in text. Please cite or delete reference.]
- Rona, P.A., and Clague, D.A., 1989. Geologic controls of hydrothermal discharge on the northern Gorda Ridge. *Geology*, 17:1097–1101.
- Strens, M.R., and Cann, J.R., 1982. A model of hydrothermal circulation in fault zones at mid-ocean ridge crests. *Geophys. J. R. Astron. Soc.*, 71:225–240.
- Zierenberg, R.A., Koski, R.A., Morton, J.L., Bouse, R.M., and Shanks, W.C., III, 1993. Genesis of massive sulfide deposits on a sediment-covered spreading center, Escanaba Trough, 41°N, Gorda Ridge. *Econ. Geol.*, 88:2069–2098.
- Zierenberg, R.A., Morton, J.L., Koski, R.A., and Ross, S.L., 1994. Geologic setting of massive sulfide mineralization in the Escanaba Trough. In Morton, J.L., Zierenberg, R.A., and Reiss, C.A. (Eds.), *Geologic, Hydrothermal, and Biologic Studies at Escanaba Trough, Gorda Ridge, Offshore Northern California*. U.S. Geol. Surv. Bull., 2022:171–197.

Figure F1. Tectonic setting of Middle Valley sedimented ridge (modified from Davis, Mottl, Fisher, et al., 1992, and Fouquet, Zierenberg, Miller, et al., 1998).

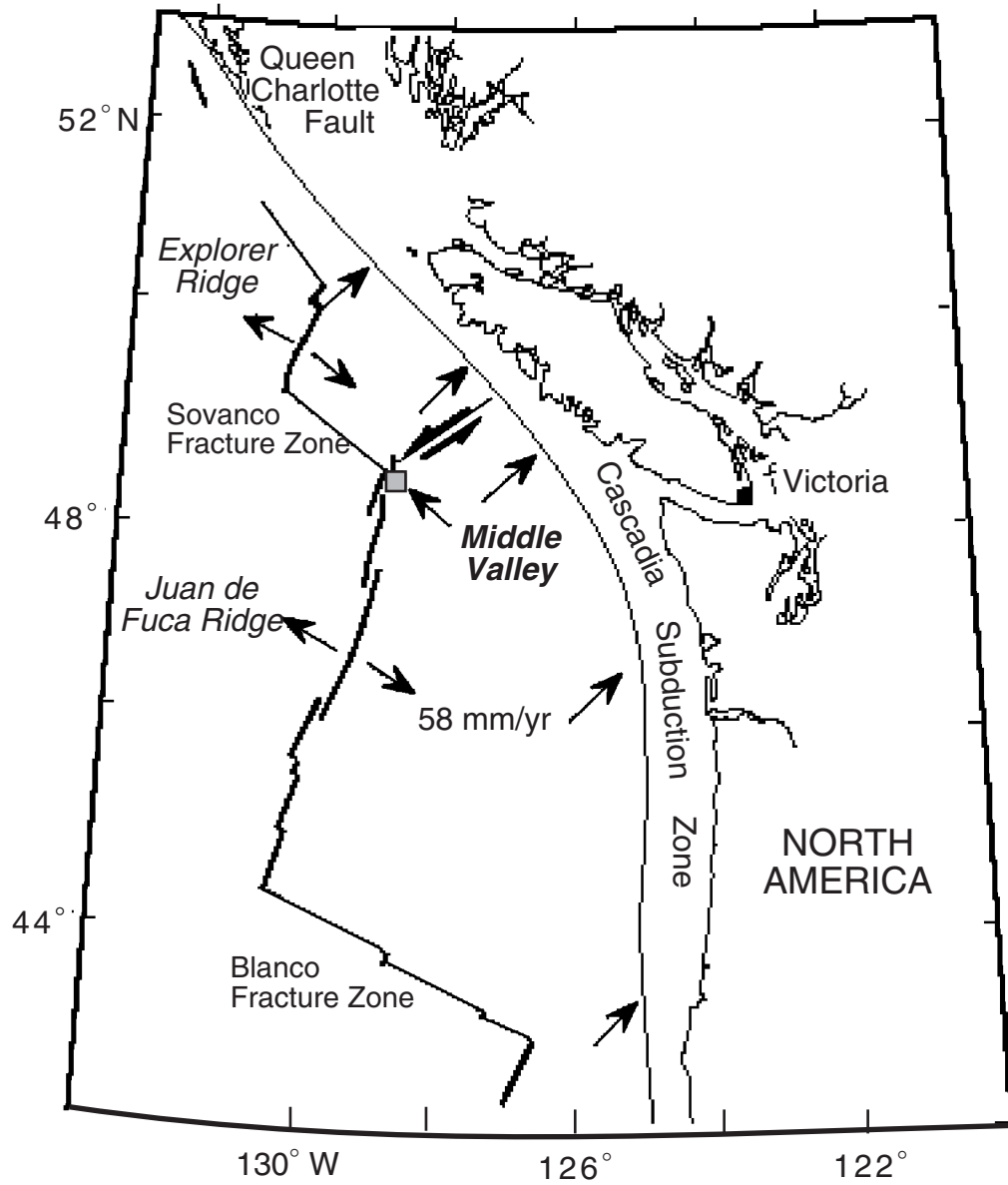


Figure F2. Location of Bent Hill and ODP Mound drill holes from Legs 139 and 169 (Fouquet, Zierenberg, Miller, et al., 1998).

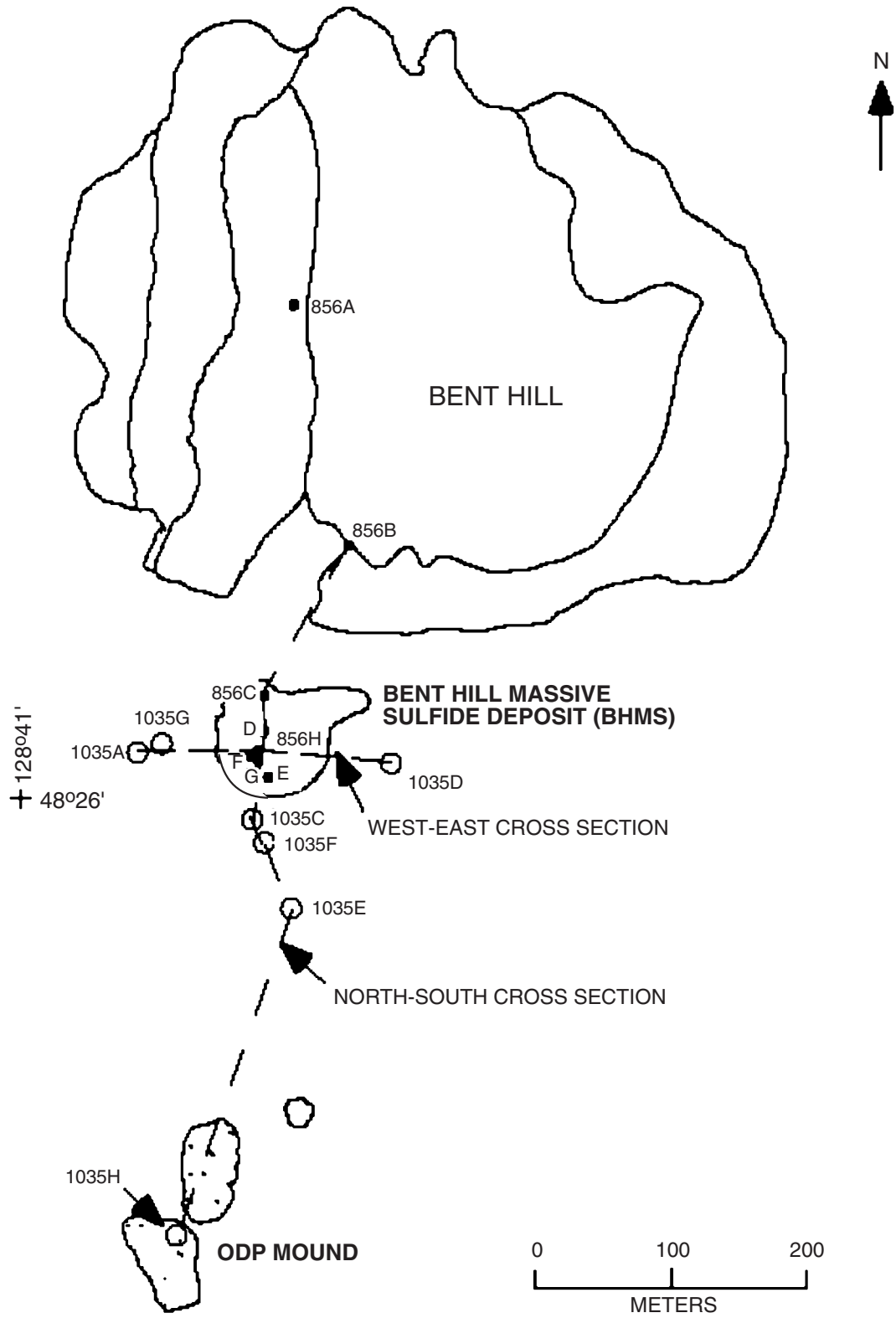


Figure F3. Log of Holes 856H, 1035F, and 1035H. A. Sample locations are marked with solid circles, and the number of samples from a specific core are noted (modified from Fouquet, Zierenberg, Miller, et al., 1998). (Continued on next page.)

A

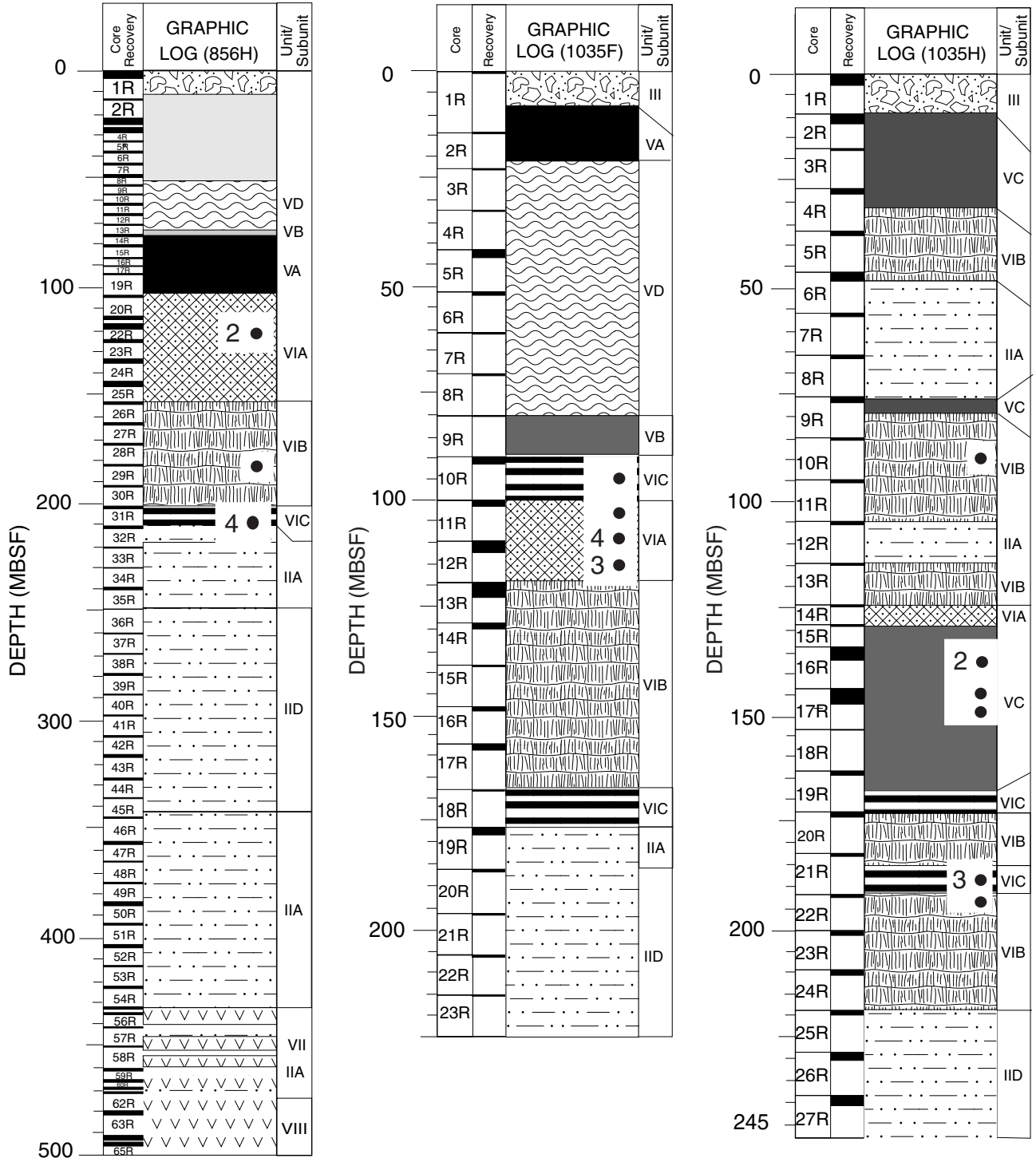


Figure F3 (continued). B. Legend.

B

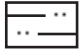





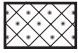



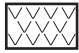
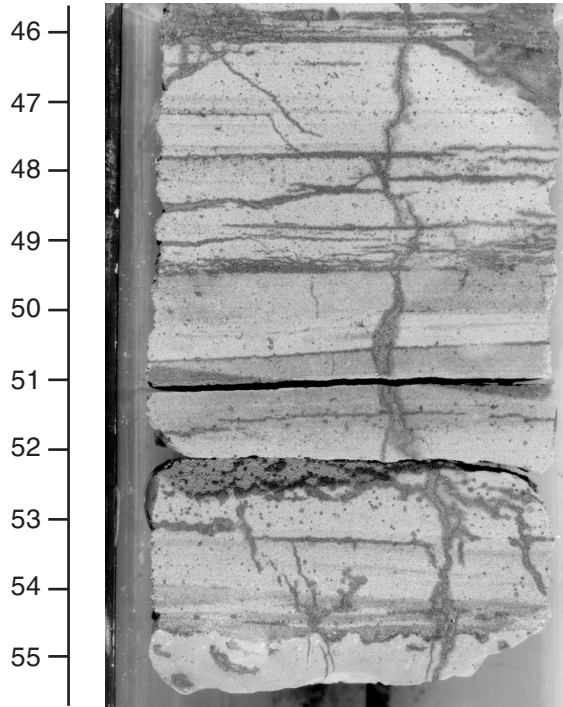
- UNIT II TURBIDITES AND HEMIPELAGIC SEDIMENTS
 (PLEISTOCENE)
-  Subunit IIA: Interbedded turbiditic sand (sandstone) and silt (siltstone), and hemipelagic silty clay (claystone)
- Subunit IID: Greenish gray, chloritic siltstone and mudstone with rare interbeds of fine-grained sandstone
- UNIT III CLASTIC SULFIDES
-  Sulfide breccia, sand, and mud interbedded with hemipelagic and turbiditic silt and sand; also includes sulfide rubble from the top of the massive sulfides (Unit V)
- UNIT V MASSIVE AND SEMIMASSIVE SULFIDES
 (>50% SULFIDE)
-  Subunit VA: Fine-grained pyrrhotite-sphalerite-isocubanite-chalcocopyrite (Type 1, Leg 139)
-  Subunit VB: Fine-grained pyrite-pyrrhotite-magnetite-sphalerite-isocubanite-chalcocopyrite (Types 2, 3, and 4, Leg 139)
-  Subunit VC: Sphalerite-pyrrhotite-pyrite-magnetite
-  Subunit VD: Colloform and vuggy pyrite (Type 5, Leg 139)
- UNIT VI SULFIDE FEEDER ZONE AND
 MINERALIZED SEDIMENTS
-  Subunit VIA: Sulfide-veined sediment (10%–50% sulfide)
-  Subunit VIB: Sediment with sulfide veins and/or impregnations (2%–10% sulfide)
-  Subunit VIC: Sulfide banded/impregnated sediment (10%–50% sulfide)
- UNIT VII BASALTIC SILLS
-  Basaltic sills intercalated with altered hemipelagic and turbiditic sediment
- UNIT VIII BASALTIC FLOWS
- 

Figure F4. A. Pyrrhotite and sphalerite as bedding-parallel veins and replacement textures (interval 169-1035F-12R-2, 46–55.5 cm). B. Subvertical pyrrhotite-isocubanite-chalcocopyrite veins (interval 169-856H-23R-1, 100–107 cm).

A



B

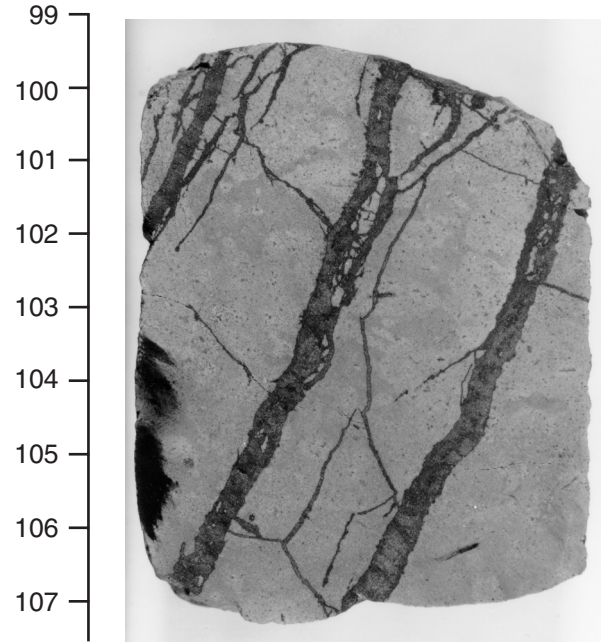


Figure F5. Backscattered electron image of quartz-lined (qtz) extension fracture infilled by pyrrhotite (po). The host rock is siltstone with chlorite alteration along grain boundaries (Sample 169-1035F-11R-2, 15–18 cm).

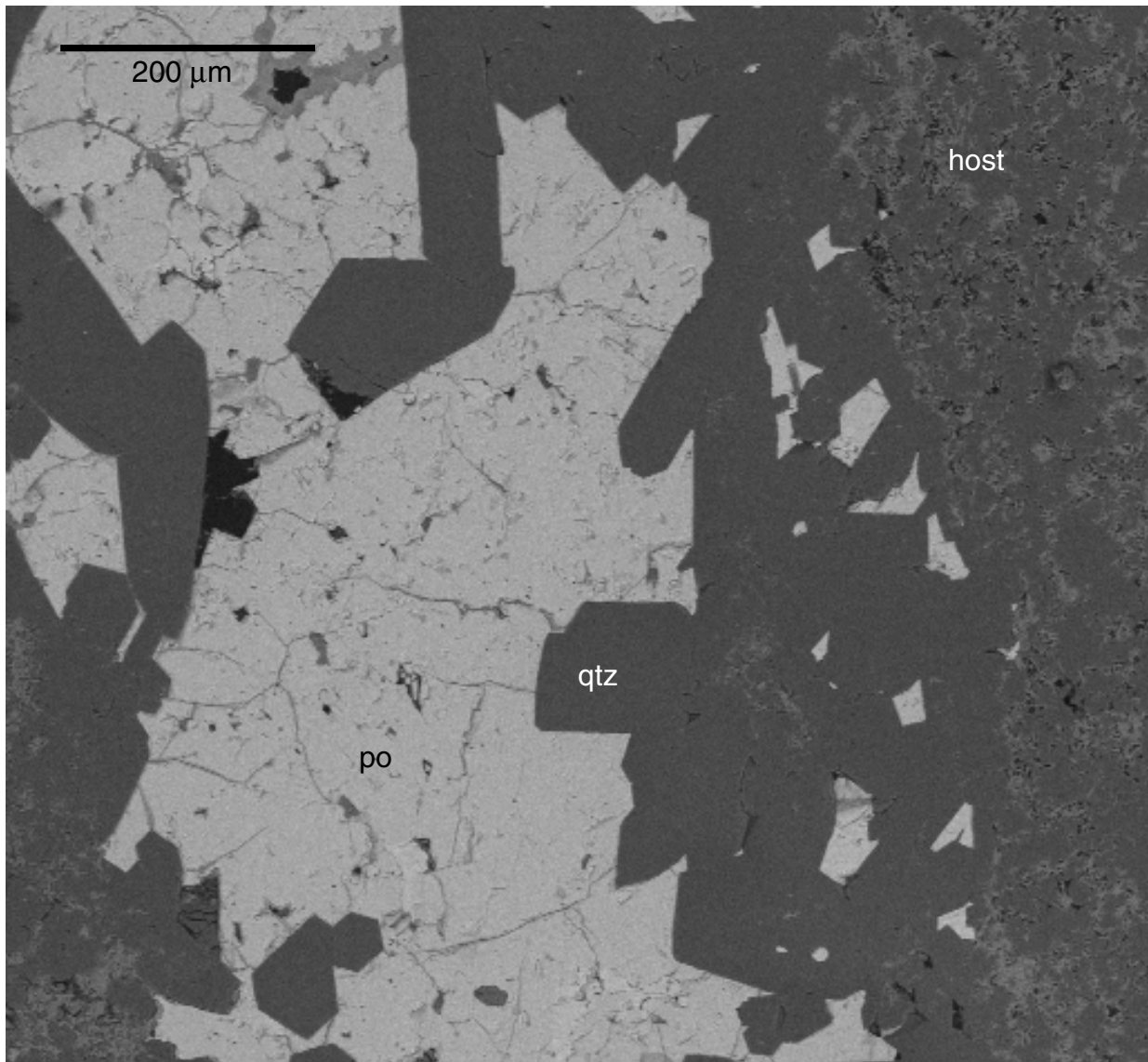


Figure F6. Backscattered image of sulfide vein assemblage at Sample 169-1035F-12R-1, 139–142 cm. Pyrrhotite (po) and sphalerite (sph) are contemporaneous. Pyrite (py) is an alteration product of pyrrhotite. Banded anhydrite (anh) borders the sulfide vein. The host rock is siltstone with chlorite. cpy = chalcopyrite.

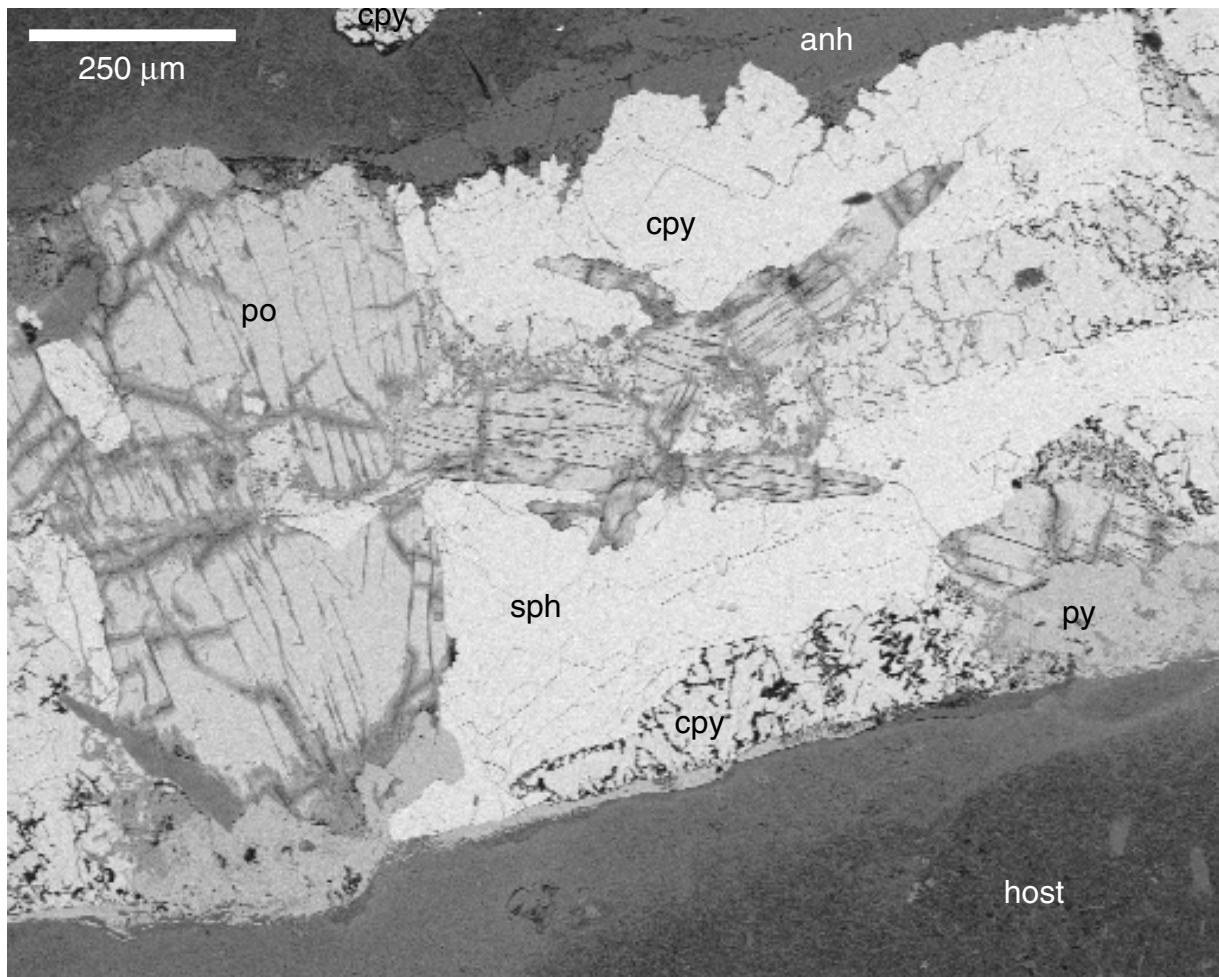


Figure F7. Backscattered electron image of chalcopyrite (cpy) blebs and veins in sulfide-veined sediment. Sediments are chlorite altered (Sample 169-1035F-12R-1, 139–142 cm). py = pyrite.

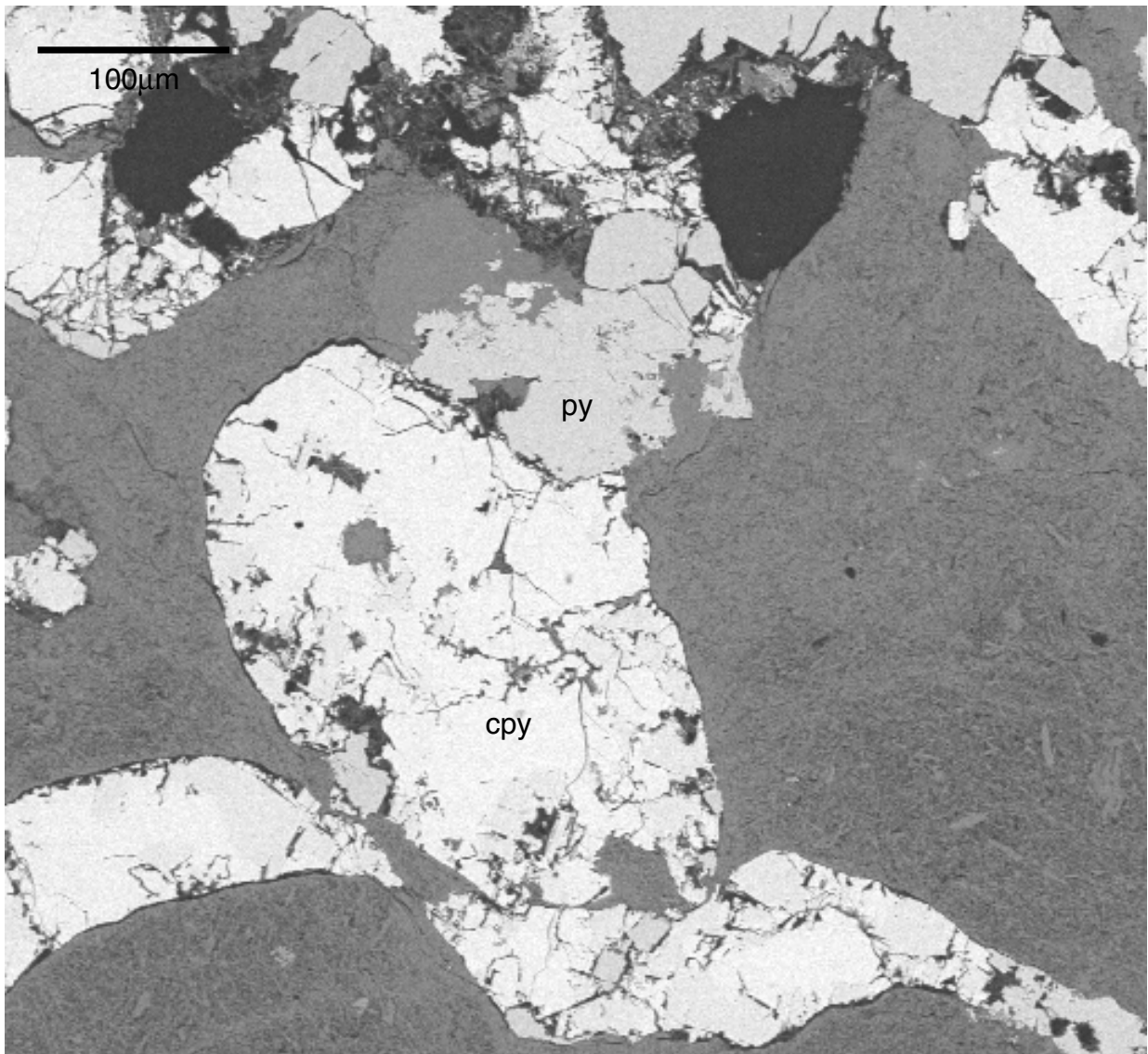


Figure F8. Core samples from Subunit VIB. **A.** Siltstone with disseminated isocubanite from interval 169-1035H-24R-1, 17–24 cm. **B.** Chalcopyrite with minor pyrrhotite replacement veins in fine-grained sandstone from interval 169-1035F-13R-1, 77–87 cm.

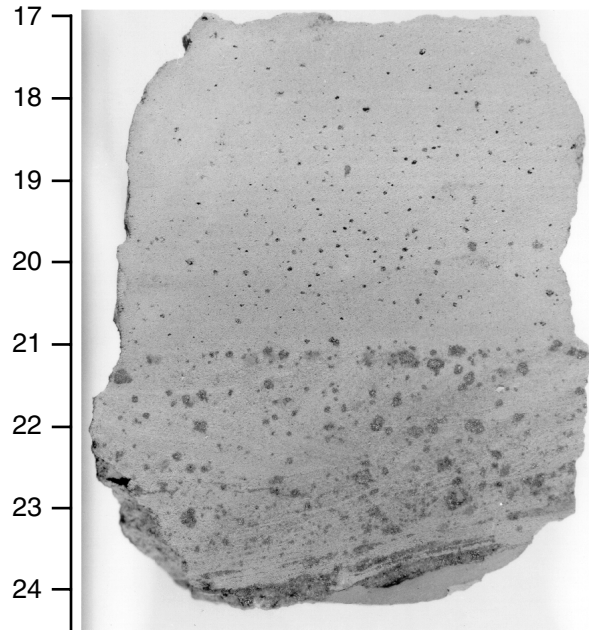
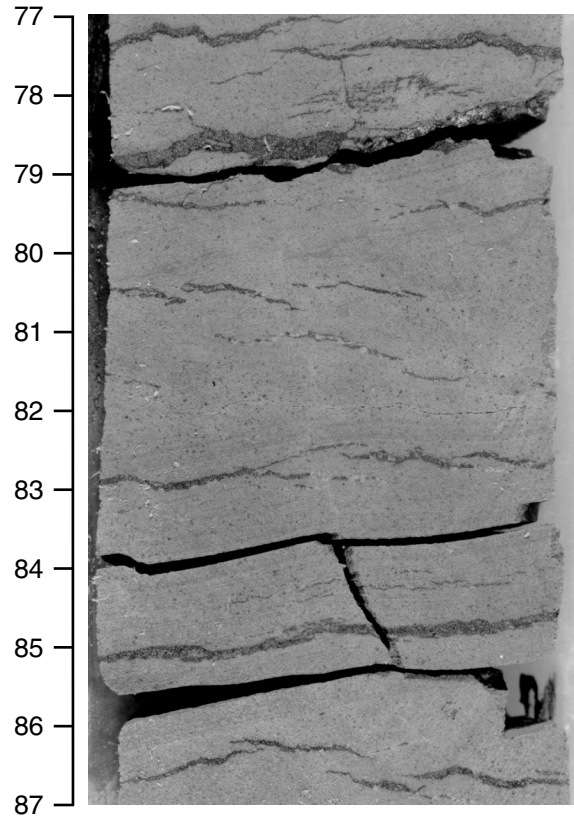
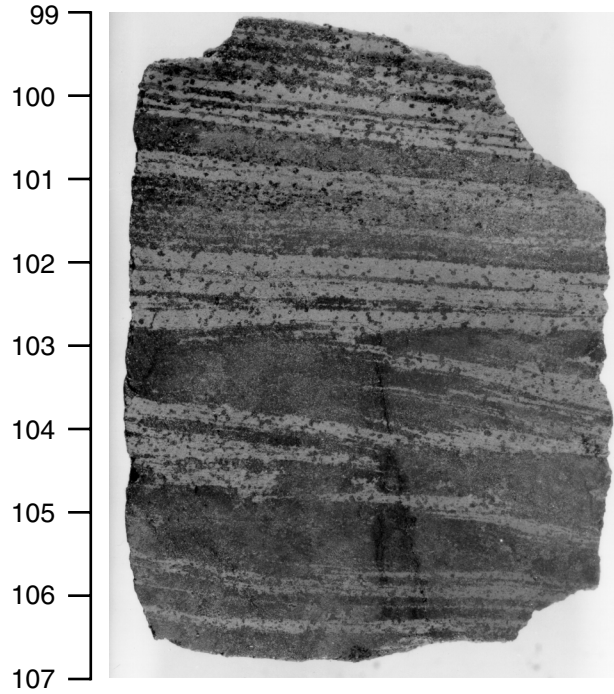
A**B**

Figure F9. Core samples from Subunit VIC. A. Cu-rich sulfide-banded cross-laminated sandstone (interval 169-856H-31R-1, 99–106.5 cm). B. Sulfide-banded sandstone where fibrous chlorite replaced detrital quartz grains and chalcopyrite precipitated within pore spaces (interval 169-856H-31R-1, 36.5–47 cm).

A



B

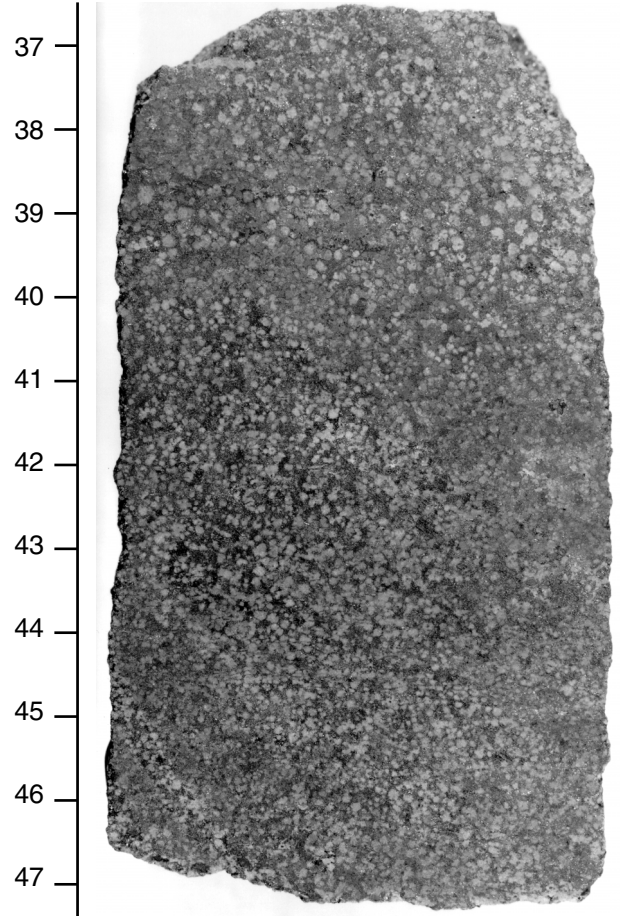


Figure F10. Chalcopyrite precipitation within sedimentary pore spaces. Fibrous chlorite replaced detrital quartz grains (Sample 169-856H-31R-1, 31–34 cm). Scale bar = 1 mm. cpy = chalcopyrite.

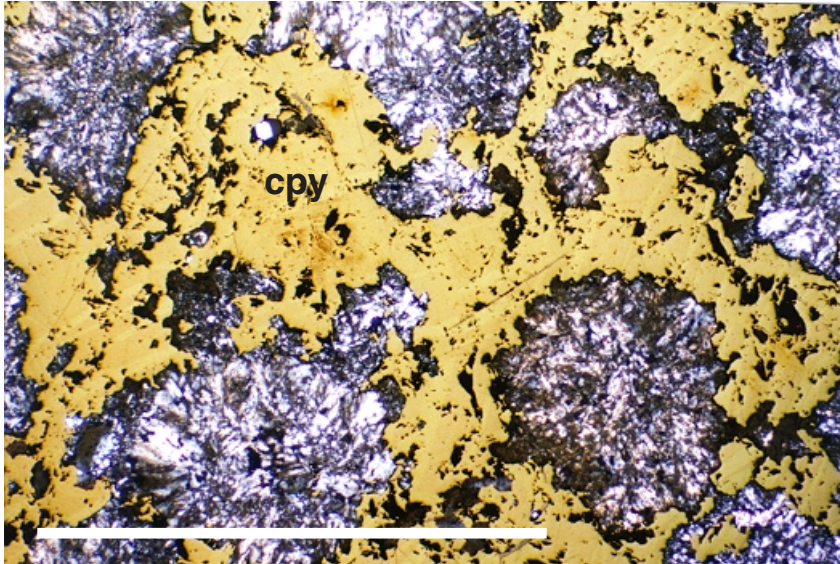


Figure F11. Pyrrhotite (po) replacement along pyrite (py) grain boundaries (Sample 169-1035H-17R-1, 119–122 cm).

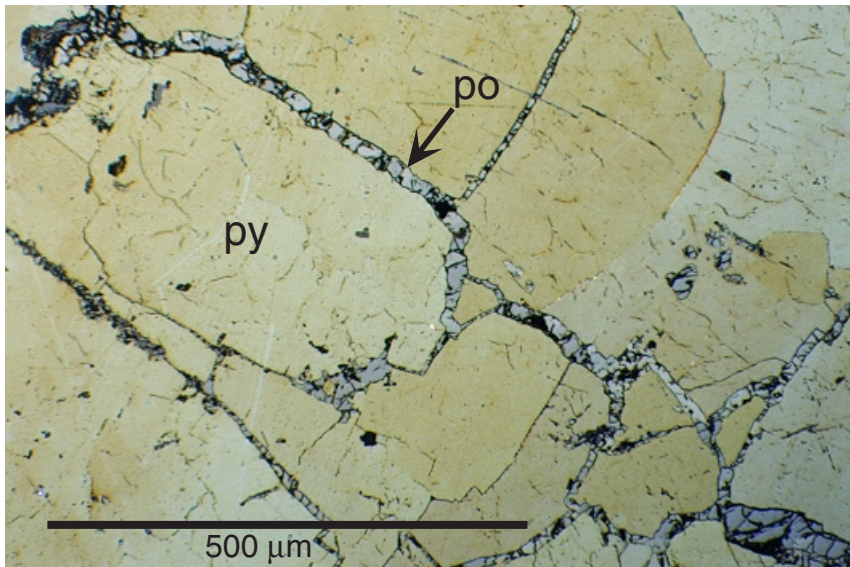


Figure F12. Vein density with depth and the representative lithology of the host rock based on core logs (Fouquet, Zierenberg, Miller, et al., 1998). Host rock is defined as the type of sedimentary rock and does not include volume percent of sulfides. The greatest vein density in Holes 856H and 1035F correspond to mudstone and siltstones. In Hole 1035H vein density corresponds to sulfide units. Note that vein density within the massive sulfides is suspect because massive sulfide may be 100% veins.

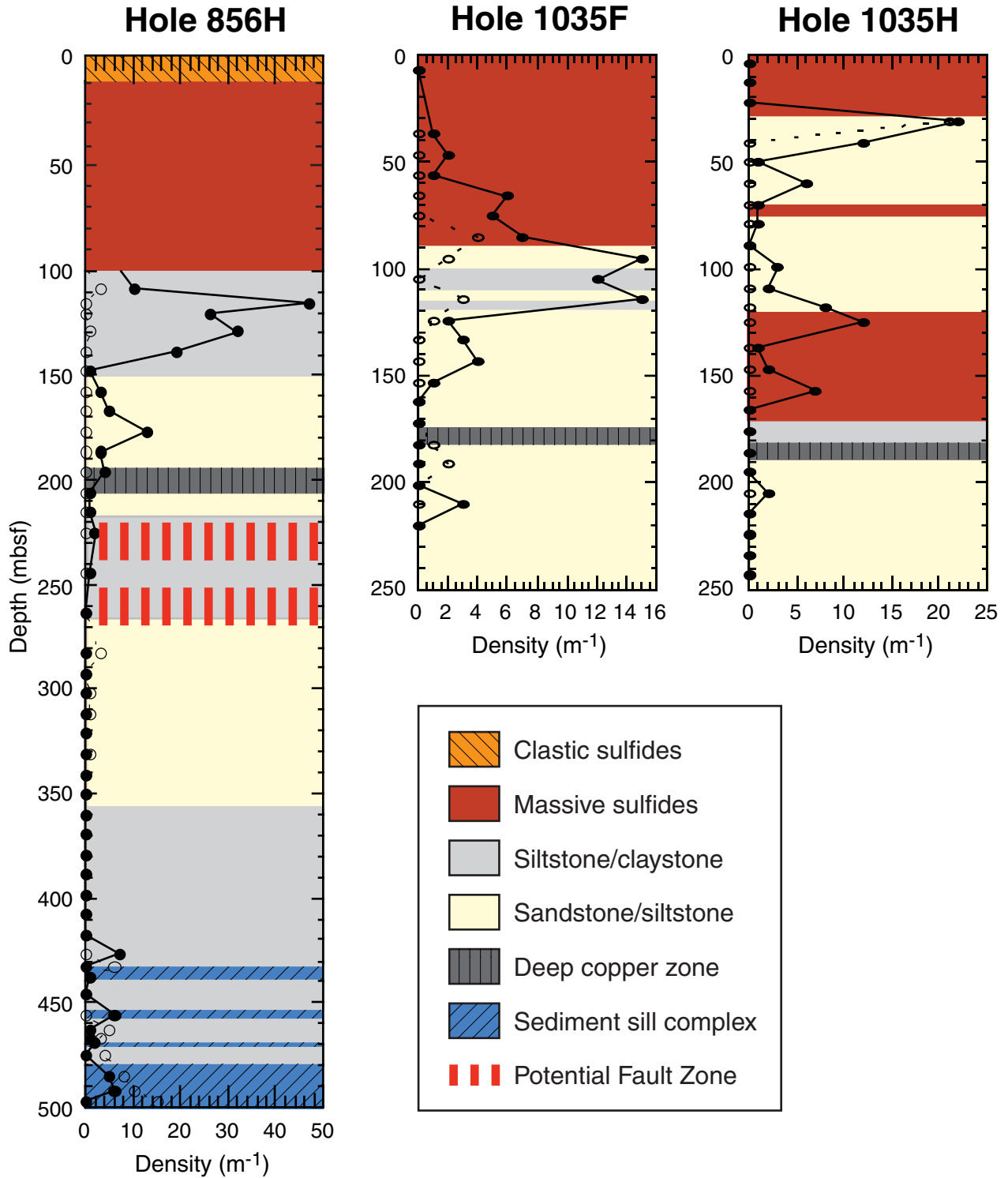


Figure F13. Hydrothermal circulation model sketched along an east-west cross-section looking north. Hydrothermal fluids flow from basalt basement through a fault conduit. As the fluids reach the surface they enter the permeable sandy turbidite units and conductively cool. Sulfide minerals precipitate within the sedimentary pore structure. In the less permeable hemipelagic mud- and clay-rich layers, hydrothermal fluids are focused through fractures.

